

Research Summaries (after joining RCAS)

The theme of this research group can be divided into two parts.

- 1) Surface and Interface Sciences: by considering and tailoring the interfacial properties, nano-sized materials are synthesized from a bottom-up approach and are used in opto-electronic applications.
- 2) Analysis and Imaging of Soft Matters: based on surface analysis techniques that characterize surface and interface properties, a series of novel techniques are developed to analyze the structure inside organic electronics directly.

While exploring biological applications currently (see current and future directions), numerous accomplishments that relate to fabrication of materials and opto-electronic applications have been made and are summarized below.

1) Surface and Interface Sciences

Synthesis of 1D Materials

For ease of processing, anodic aluminum oxide (AAO) is used widely as a structure-directing template for preparing nanotubes. These processes, however, either require a vacuum apparatus or consist of filling the template with a pre-existing solid synthesized in separate steps. Another general approach to prepare nanowires is to electroplate materials inside the template after the evaporation of electrodes on the AAO template. To further simplify the preparation, a single-step direct deposition of oxides into the template under near-ambient conditions is required. Using AAO and carefully selected solution chemistry, precursor ions are adsorbed on the inner surface of the template. After *in situ* hydrolysis reactions, stoichiometric SrTiO_3 and BaTiO_3 nanowire and nanotubes are synthesized from aqueous solutions without pre-existing solids or an electric field (**Figure 1**, *Inorganic Chemistry* **2008**, 48, 681-686).

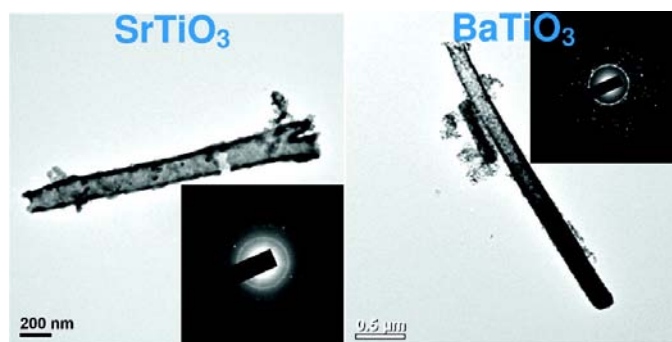


Figure 1. SrTiO_3 and BaTiO_3 nanotubes synthesized using an AAO template. Parameters including solution pH, precursor concentration, deposition temperature, and surface properties of AAO are tailored to achieve a stoichiometric composition.

Starting with a mesoporous Al₂O₃ support, TiO₂ was coated using a liquid-phase deposition. XPS showed up to 1:1 Ti³⁺:Ti⁴⁺ in the system. The Ti³⁺ in this system is found to be stable in air for an extended period of time. The catalytic oxidation of CO was used to evaluate the performance of the catalyst. The Ti³⁺-free reference catalyst shows no activity for the oxidation whereas 21.5% conversion was observed with the catalyst containing 1:1 Ti³⁺:Ti⁴⁺ at 80°C.

Table I. Ti³⁺/Ti⁴⁺ ratio, surface area, and catalytic activity of prepared catalysts.

| | Surface area (m ² /g) | Binding energy of Ti ⁴⁺ (eV) | Binding energy of Ti ³⁺ (eV) | Ti ³⁺ /Ti ⁴⁺ ratio | Conversion (%) |
|---|-------------------------------------|--|--|---|----------------|
| MP-TiO ₂ /Al ₂ O ₃ | 157 | 459.1 | --- | 0 | 0 |
| TiO ₂ /MP-Al ₂ O ₃ | 259 | 459.0 | --- | 0 | 0 |
| LD-60TiO ₂ /MP-Al ₂ O ₃ | 303 | 458.6 | 456.8 | 0.52 | 21.5 |
| LD-80TiO ₂ /MP-Al ₂ O ₃ | 281 | 458.6 | 456.8 | 0.24 | 10.8 |
| LD-100TiO ₂ /MP-Al ₂ O ₃ | 271 | 458.6 | 456.8 | 0.16 | 7.1 |
| LD-200TiO ₂ /MP-Al ₂ O ₃ | 270 | 458.6 | 457.4 | 0.09 | 5.2 |
| LD-400TiO ₂ /MP-Al ₂ O ₃ | 252 | 458.8 | --- | 0 | 0 |
| LD-600TiO ₂ /MP-Al ₂ O ₃ | 231 | 458.8 | --- | 0 | 0 |

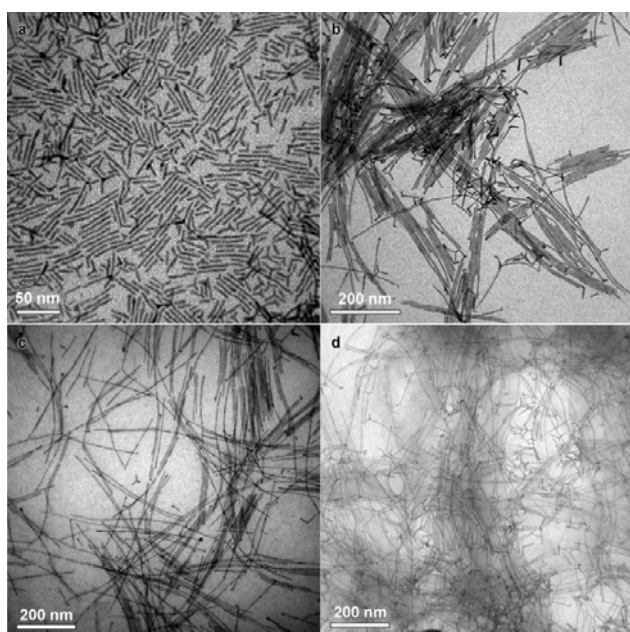


Figure 2. TEM images of CdS nanocrystals synthesized at different temperatures of **a)** 280°C, **b)** 315°C, **c)** 320°C, and **d)** 330°C.

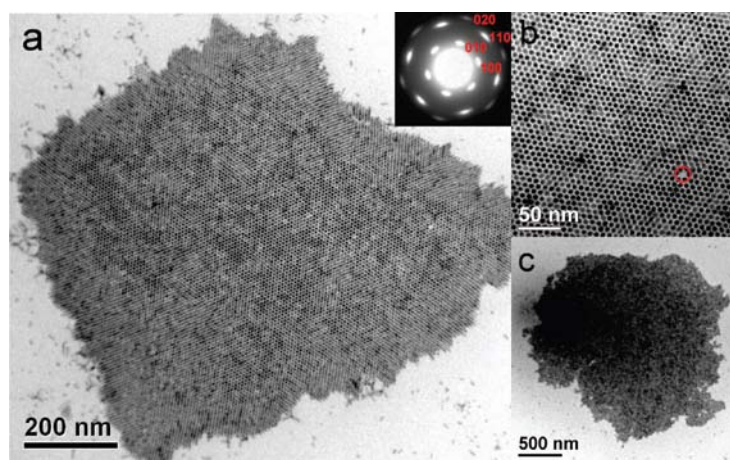


Figure 3. **a)** TEM image of TDPA- and TOP-capped CdS nanorods with self-assembled organization in large scale. The inset shows the diffraction pattern of the bundle. **b)** TEM image of bundled-up CdS nanorods under higher magnification. **c)** An extended TEM image of self-assembled CdS nanorods.

Synthesis of II-VI semiconducting nanowires also draws significant attention due to the unique properties of the resultant constructs. As an alternative to well-established VLS techniques, the liquid phase anisotropical growth of nanowires was explored. By tuning the surfactant and reaction temperature,

CdS nanowires (**Figure 2**, *Small* **2007**, *3*, 1882-1885) and self-aligning nanorod arrays (**Figure 3**, *ACS Nano* **2008**, *2*, 750-756) are fabricated without the use of templates (in collaboration with Prof. P.-T. Chou of NTU).

Ordered Arrays of 1D Nanomaterials

As an n-type semiconductor and for potential applications in solar cells, different morphologies of single crystalline ZnO was deposited from aqueous solutions (*Journal of Physical Chemistry C* **2008**, *112*, 1498-1506). In particular, the array of ZnO nanowires on transparent electrodes was demonstrated as a photoelectrode for solar cells (**Figure 4**, *Crystal Growth and Design* **2007**, *7*, 2467-2471, in collaboration with Prof. Y.-F. Gao of Musashi Institute of Technology). By anodizing titanium metal, an ordered array of TiO₂ nanotubes was prepared on an ITO surface. Using this porous structure as a photoelectrode, polymeric inverted solar cells were fabricated, and a power conversion efficiency of 2.71% was achieved (**Figure 5**, *Nanotechnology* **2008**, *19*, 955202, in collaboration with Dr. C.-W. Chu of RCAS).

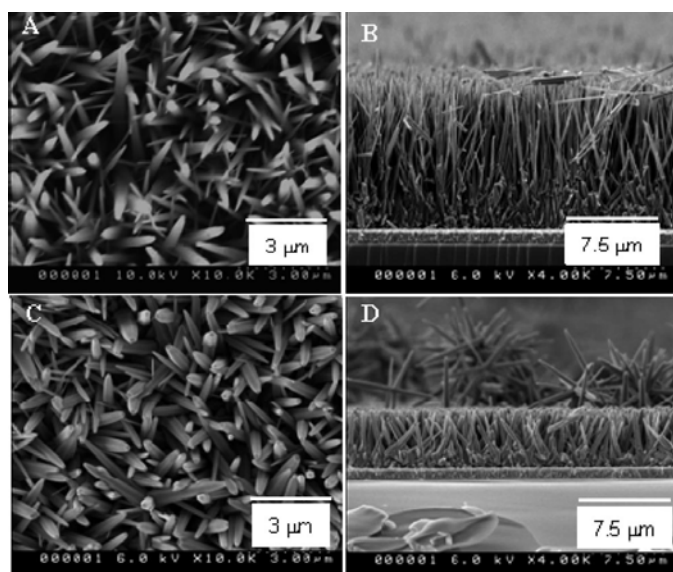


Figure 4. SEM micrographs of ZnO nanowire films prepared with different amounts of ammonia. (A, B) 5 mL; (C, D) 2 mL.

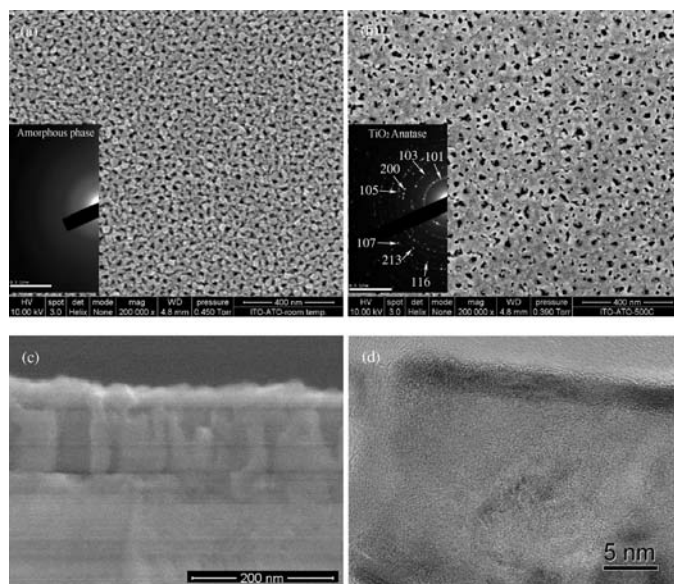


Figure 5. TiO₂ nanotube arrays: (a) SEM top view of a sample without calcination; (b) top view and (c) cross-sectional SEM images of sample after heat treatment at 500°C; (d) TEM lattice image of calcined nanotube arrays. The insets in (a) and (b) show the electron diffraction patterns of the corresponding TiO₂ layer.

Site-selective Deposition of Au on Photo-patterned SAMs

Self-assembled monolayers (SAMs) can be used to tailor surface properties and to adsorb materials selectively. Photo-lithography was used to prepare regionally separated functional groups (–NH₂

and $-\text{CH}_3$ terminal groups) of SAMs on glass, which were then used as templates for site-selective deposition. The surface potential as a function of pH was studied, and the result was used to optimize the selective deposition of metals based on electro-static considerations. The optimized pH is slightly below the isoelectric point of $-\text{NH}_2$, in which negatively-charged gold precursors are adsorbed by $-\text{NH}_2$ groups and repelled by $-\text{CH}_3$ groups, thus creating a clear pattern (**Figure 6**, *Chemistry of Materials* **2008**, *18*, 121-126).

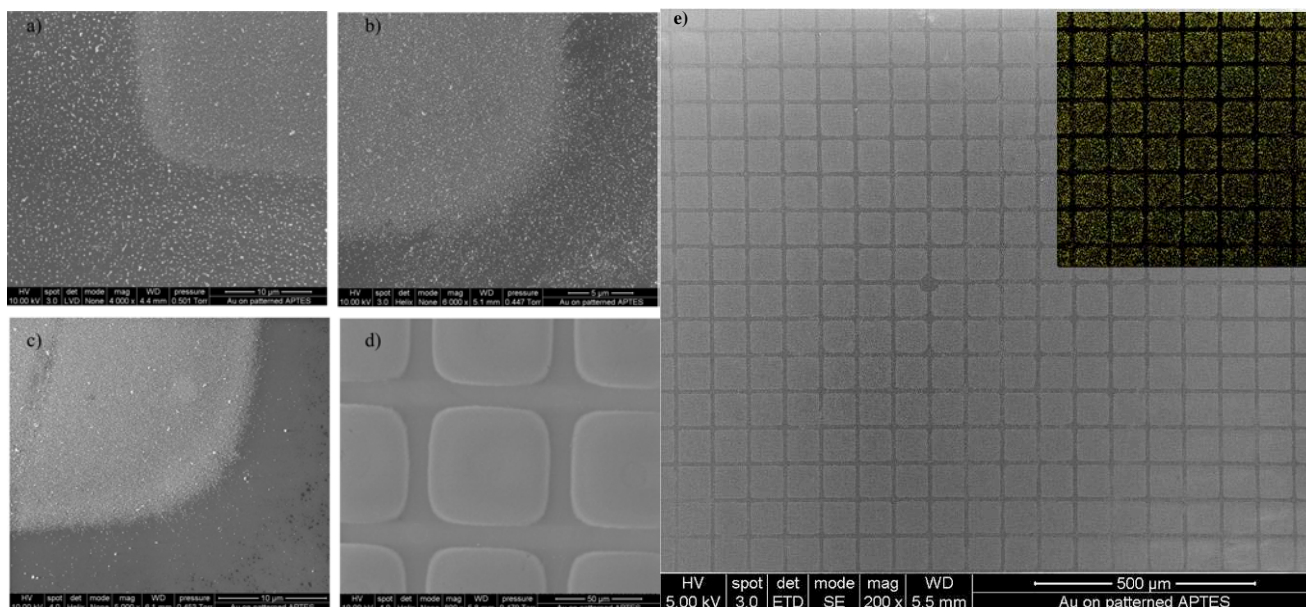


Figure 6. SEM images of the site-selective deposition of Au on UV-patterned glass substrates at **a)** pH 4.5, **b)** pH 5.5, and **c)** pH 6.5; **e)** low-magnification view of **d)**, the inset shows the XEDS mapping.

Nanodot-Enhanced Organic Light Emitting Diodes (in collaboration with Prof. J.-H. Jou of NTHU)

Polysilicic acid nanodots were doped into the hole-transporting layer of an OLED (*Advanced Functional Materials* **2008**, *18*, 121-126). Because of a more balanced carrier-injection, pure white light-emitting devices with up to a 3.5 \times higher efficiency were fabricated (*Organic Electronics* **2008**, *9*, 291-295). To gain more knowledge of how the polysilicic nanodots (PNDs) affect the carrier transportation, the surface of the PNDs were modified with amino (Am-), vinyl (V-), and alkyl (Al-) moieties in addition to the intrinsic hydroxyl (H-) functional groups. The enhancement in device efficiency is controlled by the magnitude of surface charge and is independent to the sign of the charge and the bandgap of the light emitting dye (**Figure 7**, *ACS Nano*, revised).

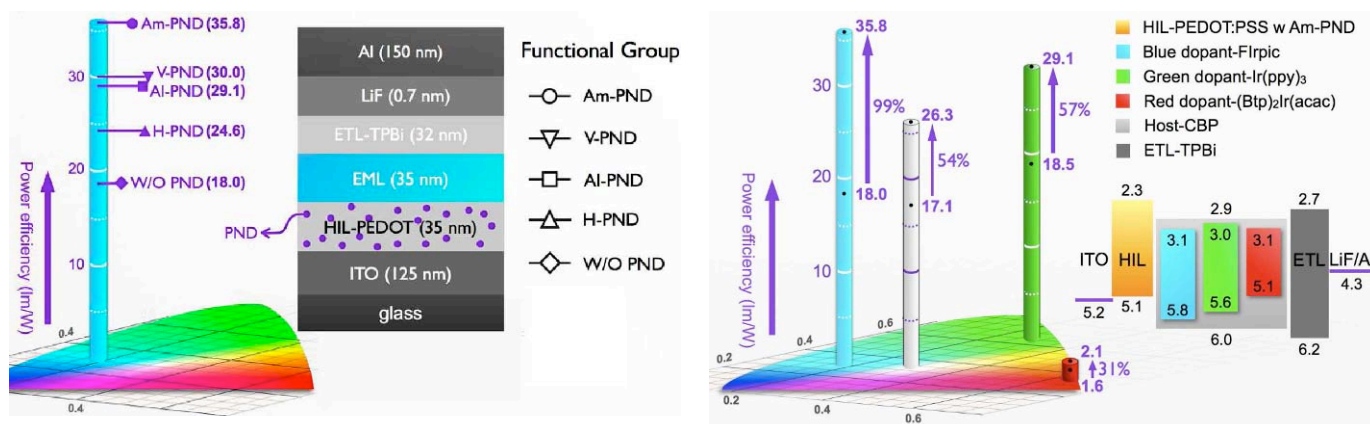


Figure 7. Incorporation effects of PNDs with various surface functional group on the power efficiency of OLED devices.

Self-Assembled Monolayers with Mixed Functional Groups

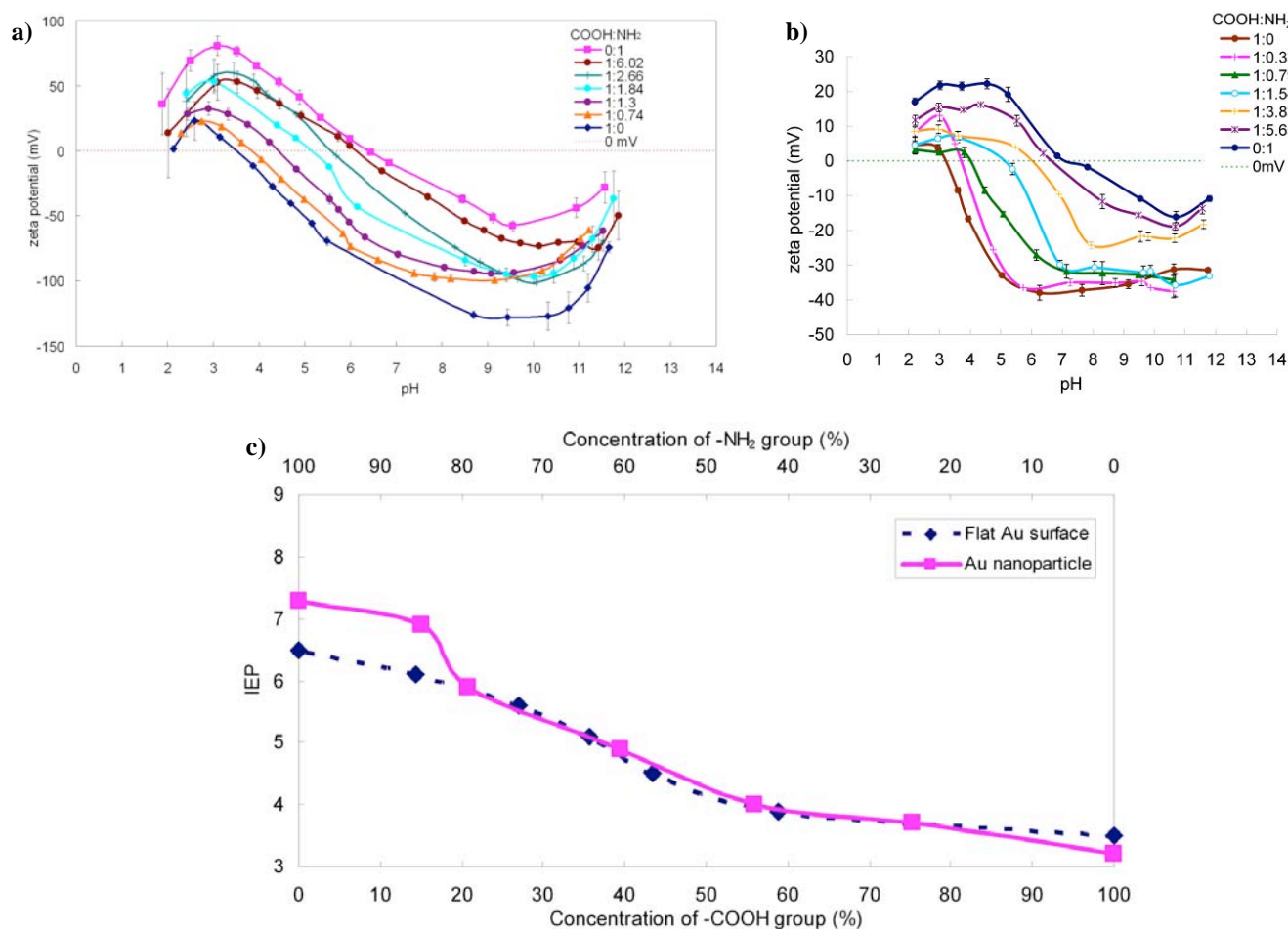


Figure 8. Zeta-potential as a function of pH for **a)** a flat Au surface and **b)** Au nanoparticles modified with various ratios of surface functional groups; **c)** IEP of the surface as a function of surface composition.

Carboxylic acid- and amine-bearing SAMs hydrolyze to carboxylate anions and ammonium cations in an electrolyte solution and yield two distinct IEP values. By mixing these functional groups on a substrate, the opposite charges can cancel each other out, and arbitrary IEP values of flat Au (**Figure 8a**, *Physical Chemistry Chemical Physics* **2009**, *11*, 6199-6204) and Au nanoparticles (**Figure 8b**, *Journal of Colloid and Interface Science* **2009**, *340*, 126-130) between the extremes defined by amine and carboxylic acid

could be achieved. These zeta-potentials are measured using independent techniques of streaming potential and dynamic light scattering and can be compared (**Figure 8c**).

Degradation of Self-Assembled Monolayers on Au

The quality of SAMs is affected significantly by the deposition conditions. By simply adding HCl to the deposition solution, a high quality amine-SAM is obtained. Using various surface analytical techniques, including contact angle analysis, x-ray photoelectron spectroscopy (XPS), and secondary ion mass spectrometry (SIMS), the hydrophilic amino group was found to slowly oxidize to a hydrophobic nitroso group even under ambient conditions. As a consequence, the surface potential (and hence, the isoelectric point) of the SAM surface changed significantly. These changes were monitored with an electrokinetic analyzer (**Figure 9**, *Journal of Physical Chemistry*, revised). These change in surface properties can be suppressed by isolating the specimen from ambient light or air indicating the degradation is a photo-oxidation process.

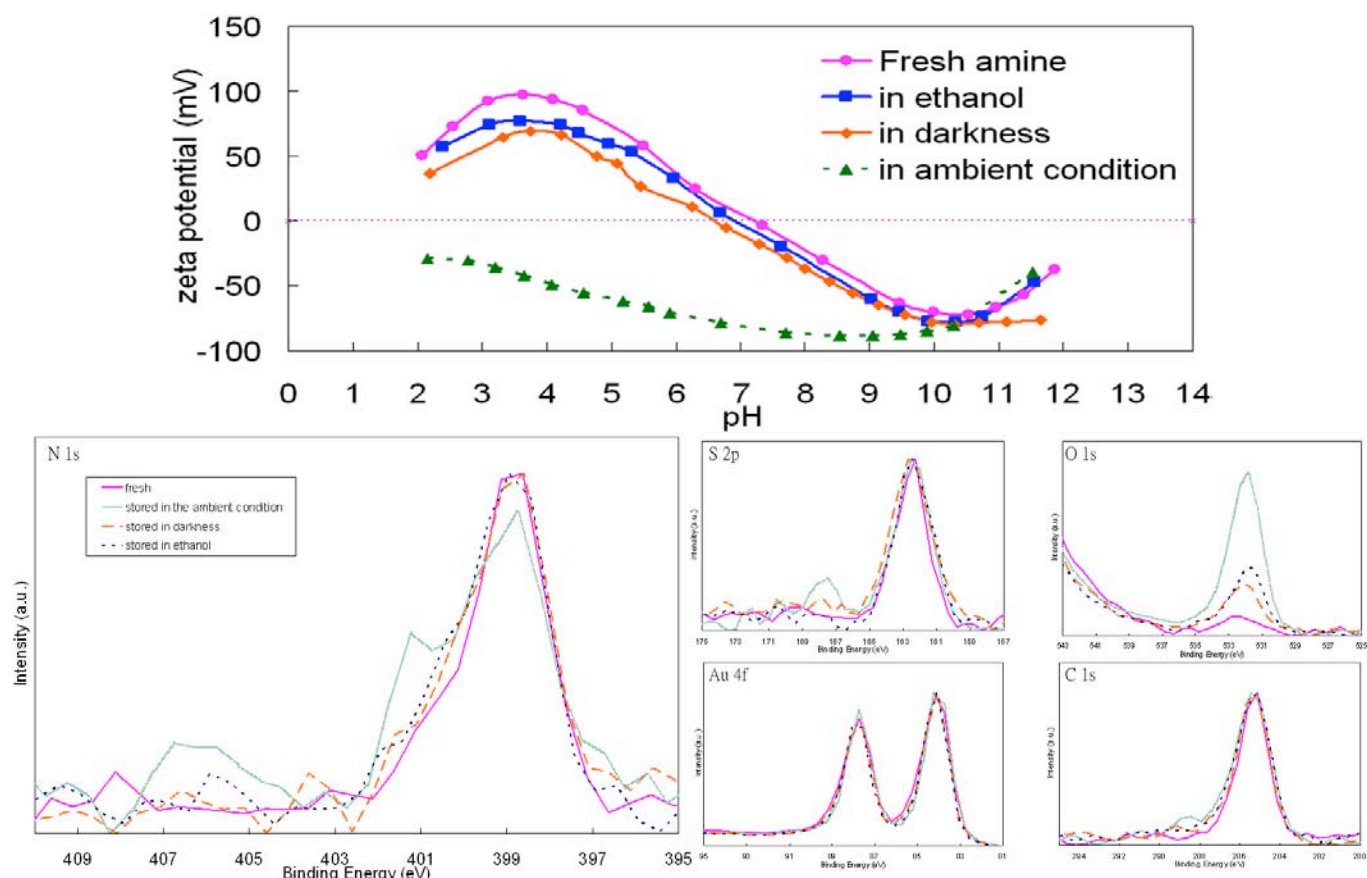


Figure 9. Zeta potential and XPS spectra of amine-SAMs stored under different conditions.

2) Analysis and Imaging of Soft Matters

XPS Depth Profiling of Organic Materials using Cluster Ion Beam

Probing the distribution of organic molecules below a surface is proven to be difficult. For example,

due to the amorphous nature and weak contrast, cross-sectional electron microscopes cannot provide reliable results. XPS depth profiling using atomic-ion-beam sputtering has been generally used to probe the distribution of inorganic materials below a surface. However, because ion-beams can induce chemical transformations, so that such a technique cannot be applied to organic materials. For the first time, by using *in situ* cluster (C_{60}^+) ion sputtering in XPS, multi-layered organic thin-films including organic LED devices and organic-inorganic hybrid thin-films were profiled without apparent damage to the chemical structure (*Analytical Chemistry* **2008**, *80*, 501-505). The carbon deposition associated with bombarding the specimen with C_{60} that causes a non-constant sputtering rate and limited sampling depth was overcome with a co-sputtering of C_{60}^+ and low-energy Ar^+ ion beams (**Figure 10**, *Analytical Chemistry* **2008**, *80*, 3412-3415). This co-sputtering technique was later adopted by instrument manufacturers and has become a standard instrument operation condition. This result is also included in review articles and textbooks. The fundamental understanding of why this technique worked was also studied (*Applied Surface Science* **2008**, *255*, 2490-2493), and no apparent benefit in analyzing inorganic materials due to the roughened surface after cluster sputtering was found (*Analyst* **2009**, *134*, 945-951).

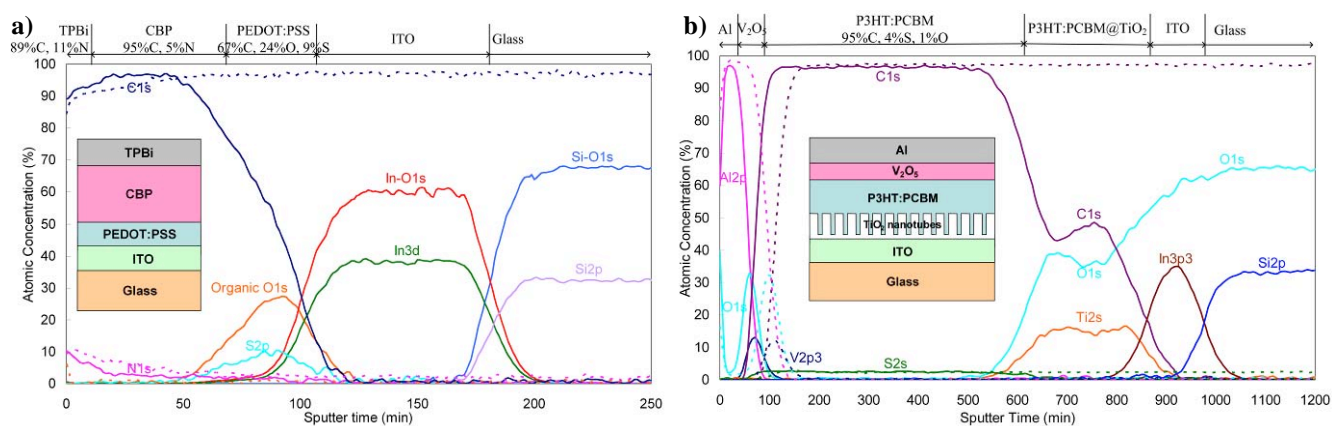


Figure 10. XPS depth profile of an **a)** OLED (specimens are provided by Prof. J.-H. Jou) and **b)** polymeric solar cell (specimens are provided by Dr. C.-W. Chu) using C_{60}^+ (dotted lines) and mixed C_{60}^+ - Ar^+ (solid lines) sputtering.

Structural Analysis of OLED Devices (specimens are provided by Prof. J.-H. Jou)

It is known that the fabrication process affects the resultant device efficiency significantly. Contrary to general expectations, it was found that spin-coating of an emissive layer consisting of a host-guest mixture results in significant phase segregation as a function of depth. On the other hand, a thermally-evaporated layer is more homogeneous with respect to depth. Such a change in the microstructure dramatically affects the charge-injection and charge-transportation and also leads to an

3.5× difference in device efficiency (**Figure 11**, *Organic Electronics* **2009**, *10*, 459-464; *Chemistry of Materials* **2009**, *21*, 2565-2567).

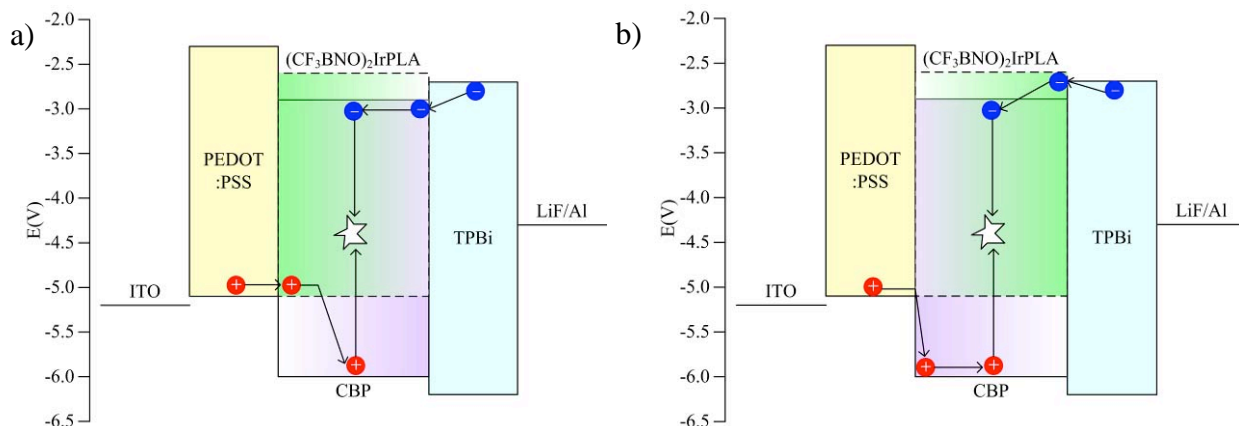


Figure 11. Energy diagram and the route of charge carriers of an OLED with EL prepared with **a)** spin-coating and **b)** thermo-evaporation. The shade of CBP and $(CF_3BNO)_2IrPLA$ indicates the relative concentration determined using C_{60}^+ depth profiling.

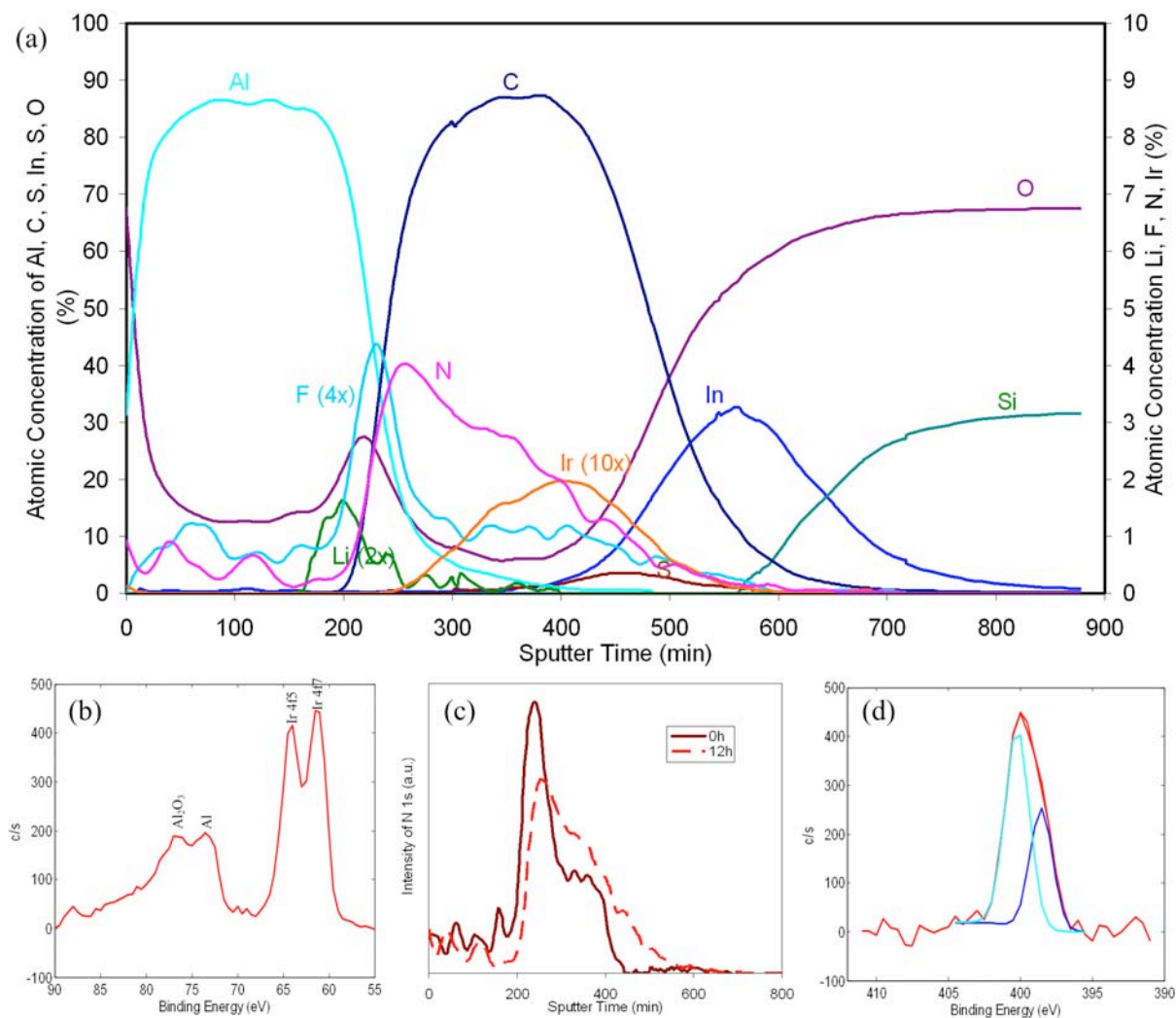


Figure 12. **a)** XPS elemental depth profiles of an OLED device operated at 5 V forward bias for 12 h. **b)** Ir 7f and Al 2p spectra of an aged device extracted between 350-500 min. **c)** N distribution before (solid line) and after operation for 12 h (dashed line). **d)** N 1s spectrum of an aged device extracted between 350-500 min demonstrating the electron-migration of electron-conducting TPBi molecules into the light-emitting CBP layer.

This novel analytical technique has also been used to study the degradation of an organic LED

directly (**Figure 12**, *Organic Electronics* **2009**, *10*, 581-586). Currently, there are no other means that can analyze the structure of a whole organic electronic operated for different times directly. In addition to the previously proposed degradation mechanisms, a new mechanism based on the direct observation of the migration of small molecules under direct current is reported. This mechanism has never been considered before and can explain the reported results. The knowledge gained in this work is crucial to the success of organic electronics with sufficient life-times for real applications.

3D Nanostructure inside Organic Electronic Devices

To gain high spatial resolution in 3D, the sputtering technique that provided excellent depth resolution was combined with scanning probe microscopy, which has high lateral resolution. By combining different instrumental techniques like scanning electrical potential microscopy (**Figure 13**, *Analytical Chemistry* **2009**, *81*, 8936-8941, highlighted by the journal, specimens are provided by Dr. C.-W. Chu) or force modulation microscopy (*ACS Nano*, revised, specimens are provided by Prof. J.-H. Jou), the nanostructure inside organic materials can be examined at high resolution. The fabrication parameters affect the resulting nanostructure significantly. For solar-cell devices, the phase-separation inside the bulk-heterojunction provides an adequate path for the removal of charge carriers that in turn enhance the device efficiency. On the other hand, phase-separation inside light-emitting devices is less efficient in trapping the charge carriers, which leads to efficiency drops with the development of a nanostructure.

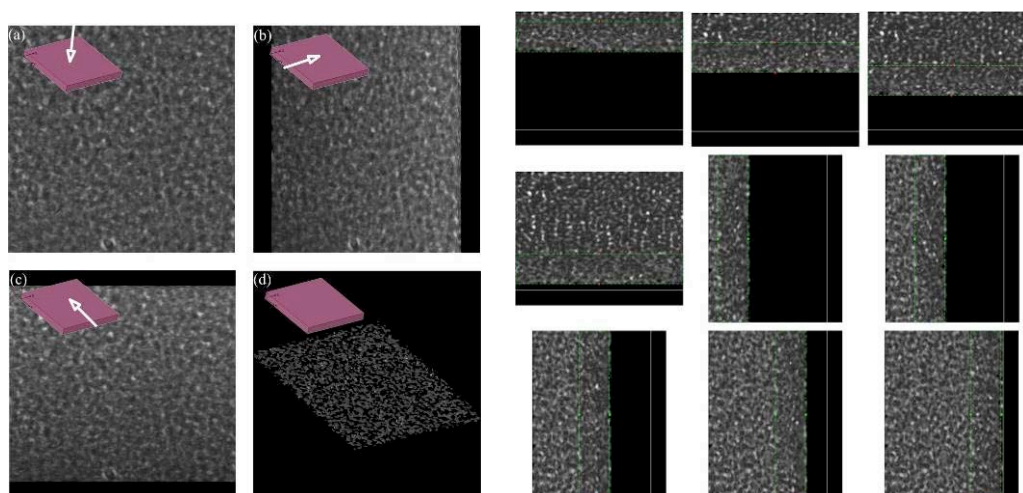


Figure 13. 3D projection and slices of the reconstructed 3D structure P3HT:PCBM

In collaboration with ULVAC-PHI, a scanning ToF-SIMS with spatial resolution of 50 nm is also demonstrated (*ACS Nano* **2010**, *4*, 833-840). Using a bulk heterojunction solar cell (**Figure 14**, specimens

are provided by Prof. J.-H. Jou) as an example, the 3D molecular distribution was obtained before and after annealing. This work revealed the important relationship between fabrication conditions, nanostructure, device architecture, and device performance.

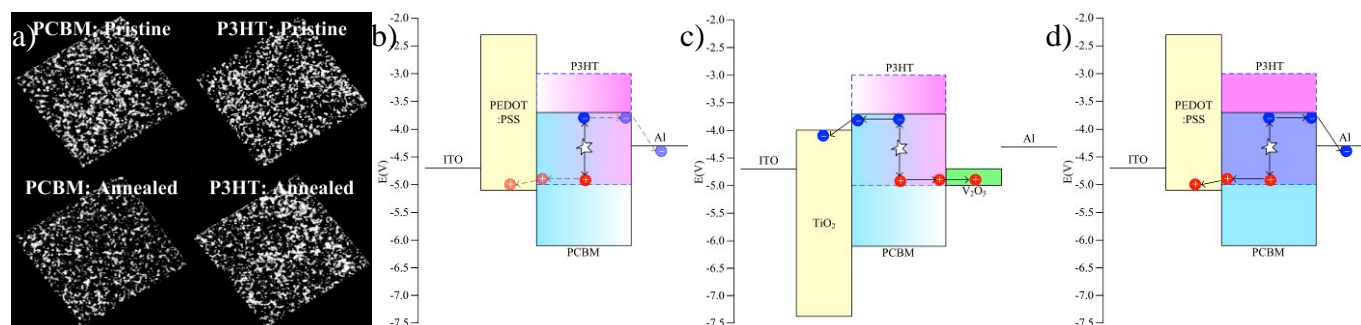


Figure 14. (a) 3D volume distribution of P3HT:PCBM blends. The theoretical energy level diagrams and carrier transportation for the pristine P3HT:PCBM blend in the (b) normal and (c) inverted device architecture and (d) the annealed P3HT:PCBM blend in the normal device structure. The shading of the color indicates the differences in concentrations.

Compared with established techniques like electron tomography, which can yield 3D nanostructures, the contrast generated by our technique is from direct physical properties instead of crystallinity that relates indirectly to the materials. Furthermore, ion sputtering has no physical limitations to the analyzable thickness. As a result, as long as the sample is stable to high-vacuum it can be studied in its original state without sample preparation that can introduce artifacts. Therefore our techniques are universal and more versatile than TEM-based techniques.